

Dynamic numerical simulation of plastic deformation and residual stress in shot peening of aluminium alloy

Himayat Ullah^{*1}, Baseer Ullah¹ and Riaz Muhammad²

¹Centre of Excellence in Applied Sciences and Technology (CESAT), Islamabad, Pakistan

²Department of Mechanical Engineering, CECOS University of IT and Emerging Sciences, Peshawar, Pakistan

(Received November 27, 2016, Revised March 8, 2017, Accepted March 15, 2017)

Abstract. Shot peening is a cold surface treatment employed to induce residual stress field in a metallic component beneficial for increasing its fatigue strength. The experimental investigation of parameters involved in shot peening process is very complex as well as costly. The most attractive alternative is the explicit dynamics finite element (FE) analysis capable of determining the shot peening process parameters subject to the selection of a proper material's constitutive model and numerical technique. In this study, Ansys / LS-Dyna software was used to simulate the impact of steel shots of various sizes on an aluminium alloy plate described with strain rate dependent elasto-plastic material model. The impacts were carried out at various incident velocities. The influence of shot velocity and size on the plastic deformation, compressive residual stress and force-time response were investigated. The results exhibited that increasing the shot velocity and size resulted in an increase in plastic deformation of the aluminium target. However, a little effect of the shot velocity and size was observed on the magnitude of target's subsurface compressive residual stress. The obtained results were close to the published ones, and the numerical models demonstrated the capability of the method to capture the pattern of residual stress and plastic deformation observed experimentally in aluminium alloys. The study can be quite helpful in determining and selecting the optimal shot peening parameters to achieve specific level of plastic deformation and compressive residual stress in the aluminium alloy parts especially compressor blades.

Keywords: shot peening; impact; finite element analysis; residual stress; plastic deformation

1. Introduction

Shot peening is a cold working surface treatment process typically used for the improvement of the fatigue strength of many critically loaded metallic parts (Meguid *et al.* 1999, Meguid and Maricic 2015). The process is widely employed for treatment of metallic components in aerospace, automotive and power generation industries. Gas turbine engine components such as turbine and compressor discs, blades and shafts, landing gear components, springs, gears, connecting rods and cam shafts are normally surface treated by shot peening (Hidayetoglu 2001, Majzoobi *et al.* 2005). In this process, the surface of the metal part is impacted with small shots at high velocities ranging from 20 m/s to 100 m/s. Shots are usually made of steel, glass or ceramic beads. As a result of striking a shot with the surface of a metal part, a small indentation is created which is surrounded by a plastic region followed by an elastic zone. As the shot rebounds, the recovery of elastic zone creates a large compressive residual stress on the surface (Majzoobi *et al.* 2005). The overlapping of these surface indentations develops a uniform compressive layer at the material surface, which squeezes the grain boundaries of the material surface together; thus significantly delaying the fatigue

crack initiation. Consequently, the fatigue life of the part can be greatly enhanced (Hong *et al.* 2008). In small aero engines, the process is employed to induce compressive residual stress field in compressor blades usually made of aluminium alloys. During operation, the blade is subjected to centrifugal loads causing tensile stress in it. The already locked compressive residual stress mitigates the magnitude of the tensile stress and hence the blade works below its yield limit with increase in safety factor and fatigue life. In this study, the thin blade is taken as a flat plate to determine the shot peening parameters for the required level of plastic deformation and residual stress in actual surface treatment of the blade. As the blade average thickness is small compared to its planar dimensions i.e., chord to average thickness and height to average thickness ratios are 17.0 and 15.0, respectively. Further, due to high velocity impact and small size of the shot, the effect of shot peening is localised. Therefore, thin aerofoil blade can be assumed as flat plate.

Both experimental and numerical techniques can be employed to predict parameters of shot peening and its influence on the target surface treatment. A wide range of experimental investigations have been carried out to evaluate the plastic deformation, residual stress distribution, fatigue life and the effect of shot, target and process parameters (Shukla *et al.* 2014, Carlos Rubio-Gonzalez 2015, Mann *et al.* 2015). Despite its usefulness, the experimental method suffers from several difficulties related to the cost and time of experimentation to evaluate the effect of each parameter on the surface treatment

*Corresponding author, Ph.D.
E-mail: uhimayat@gmail.com

(Mohamed Jebahi 2016). On the other hand, numerical technique such as finite element method is a robust tool capable to determine a range of shot peening parameters and its effect on the residual stress distribution and plastic deformation on the part surface. FE analysis can take into account the high velocity impact of a shot with the target involving nonlinearities due to the target material as well as contact of sphere with the target employing explicit dynamics solvers. The numerical simulation technique is computationally economical and very attractive. Moreover, it has the potential to predict the complex nature of the shot peening during its impact on the target surface. In recent years, with the availability of increased computational power and numerous commercial FE packages, modelling and simulation of the shot peening process has become an increasingly attractive alternative to the tedious experimentation of the process.

Regarding numerical simulation of the process, (Al-Obaid 1990) was among the pioneers to carry out 3D simulation of shot impacts employing finite element method. (Meguid *et al.* 1999, Meguid *et al.* 2002) investigated the single and multiple shot impacts using three-dimensional (3D) FE models of rigid spherical shots and metallic targets. They studied the influence of various important factors such as the shot velocity, size and shape and target's material properties on residual stress distribution in the target. Their results revealed that the influence of shot parameters was substantial than the rate of work hardening of the target. (Majzoubi *et al.* 2005) developed a three-dimensional model in explicit dynamics LS-DYNA code simulating shot peening process with multiple shots impacts. They obtained residual stress profiles and investigated the influence of shot velocity and peening coverage. (Hong *et al.* 2008, Hong 2008) developed a 3D dynamic finite element analysis of two and multiple shots impacting on a metallic component. The FE model was validated against a published study giving a good agreement. Parametric study was also conducted to study the effect of shot impacting with overlap on the induced residual stress profile in the part. (Bagherifard *et al.* 2014) conducted the mesh sensitivity study of shot peening finite element models intended at surface grain refinement. They revealed that mesh size affects both the magnitude and extent of residual stress, and equivalent plastic strain in the target material. (Chen *et al.* 2014) conducted analyses of the arc-height development in shot-peened Almen strips using the FE method. (Bhuvanaraghan 2010) employed the discrete element method for shot as a rigid body and finite element method for deformable target plate in simulating shot peening process. Recently, (Mann *et al.* 2015) determined residual stress distribution caused by a single shot on an aluminium alloy 2024 using numerical simulations in Abaqus/ Explicit. They found a good agreement between experimental and numerical results in residual stress distributions.

Although a substantial amount of numerical studies exist in the literature, still shot peening is a complex process involving multiple parameters which needs to be fully investigated in all its magnitude employing numerical techniques. Further, in industry, it is of great importance to

quantify the effect of parameters such as shot velocity, diameter and material which govern the peening process, which is very difficult and costly to predict experimentally. In majority of the above numerical studies, shots are usually modelled as discrete rigid bodies whereas few studies have modelled it as a deformable body. Normally, shots are modelled as rigid bodies when their material's stiffness, hardness and yield strength are larger than that of the target material, and deformable when both have comparable properties (Mohamed 2016). In this study, the stiffness and hardness of steel shots are larger than that of aluminium alloy target favouring the shot modelling as rigid one. However, in actual shot peening process, the shot still has a finite stiffness and thus both the shot and target can be considered as deformable bodies. Therefore, in this study, both the shot and target are elucidated as deformable bodies in FE model in order to investigate the effect of shot stiffness on the induced residual stress during shot peening process. Additionally, in practice, shot peening process consists of a large number of shots impingement on a target material randomly. To analyse all these random impacts, a large amount of computational resources as well as time is required which may make simulation of the complete process very expensive. Further, a single impact model is usually developed to predict the effect of peening parameters on the surface refinement of target material whereas multiple impact models are employed to determine the percent coverage of the target surface (Hassani-Gangaraj and Schuh 2015). Still, in these models, only a small number of shots are modelled in a deterministic way which affects their ability to analyse the actual shot peening experiment, which is practically stochastic. Therefore, this study, has focused on simulating the process by modelling both the shot and target material as deformable bodies; taking a single shot impact.

The aim of this work is to carry out numerical simulation of shot peening process to study the elastoplastic dynamic process of shots impact on an aluminium alloy target. The strain rate dependent and work hardening material behaviour of the target is considered by using Johnson-Cook plasticity model. To the authors' knowledge for the first time, the dynamic behaviour of shot peening process is elaborated by describing the time histories of force, energy, induced stress and plastic deformation of shot interaction with the target. Using FE modelling, a parametric study is also conducted to predict the effects of key parameters such as shot velocity and size on the spatial distribution of residual stress distribution and plastic deformation within the metallic target. Simulations also provided a meaningful insight into the target material's behaviour which could not be achieved experimentally. Further, the parameters predicted with simulations will be used for actual shot peening of thin compressor blades.

2. Finite element simulations

2.1 Description of FE model

Three-dimensional FE models consisting of a target

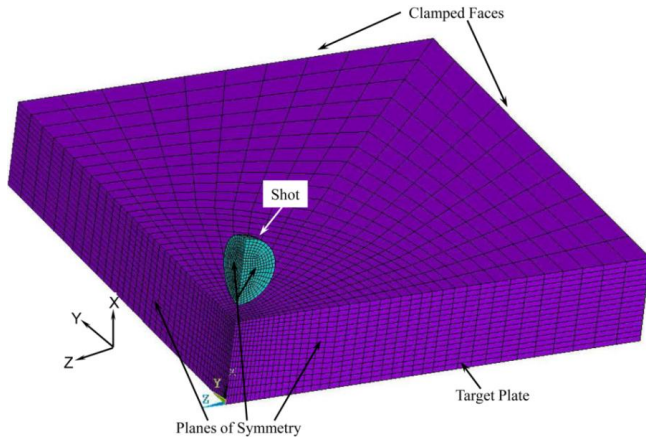


Fig. 1 3D FE model used for impact simulation

plate and shot were developed in the FE software ANSYS/LS-DYNA, with explicit algorithm to investigate impact of shot on the target. The dimensions of the target plate of 5 mm×5 mm×0.5 mm were kept constant through all the simulations whereas steel shots of diameters 0.4 mm, 1 mm and 2 mm were used. The target compressor blade/plate was made of Aluminium alloy 2618-T61, which has better properties over a range of temperatures and is usually used in applications where high strength and creep resistance are important considerations. The shot was kept just above the plate to reduce the computational time of bringing it into contact. The FE model is shown in Fig. 1. Due to symmetry of the problem, only one quarter portion of the plate as well as shot were modelled, thus reducing the computational cost. Hence, symmetry boundary conditions were applied on two planes XY and XZ of the model. The two outer sides of the rectangular target plate were restrained against displacement and rotations to represent its fully clamped conditions (Fig. 1). The base of the target was constrained in vertical X direction. The shot was free to move in vertical direction (X-axis) only and was assigned initial axial velocity in this direction.

In numerical models of shot peening process, the target plate is usually defined as deformable body whereas shot is described as a rigid body as studied in (Majzoubi *et al.* 2005, Hong *et al.* 2008, Mann *et al.* 2015). In the real world scenario, the shot can behave either rigid or deformable body depending on its stiffness and hardness as compared to target material. Although, the stiffness of the steel shot is three times greater than that of the target, here it is treated as deformable body to examine its effect on the residual stress distribution. Therefore, in the numerical implementation, a multi-body dynamics approach has been utilized, which is mostly adopted for the simulation of deformable bodies that experience large deformations during their interaction (contact). The contact between the shot and the target plate was described by a surface-to-surface general contact algorithm employing penalty method, available in LS/Dyna. The nodes on the lower half of the shot surface were selected as contact nodes whereas the nodes on the top surface of the target around the common normal were described as the target nodes (Fig. 1). The coefficient of friction used at contact between the shot

and the plate was 0.25, as proposed in (Meguid *et al.* 2002, Hong *et al.* 2008). The accurate modelling of contact problem needs that the impacting shot must not to penetrate the target. This is achieved by assigning optimum penalty stiffness to the contact pair, which depends on the relative stiffness of the contacting bodies. The use of high stiffness values result in numerical instability and solution divergence, whereas lower values result in interpenetration of the contacting bodies. Therefore, this stiffness was optimised by conducting several runs of the FE model. Further, in explicit dynamics solutions, the stiffness type penalty increases stiffness of the system, which increases the speed of sound at least locally (Belytschko 1991, Hetherington 2011). Hence, the critical time step, which is inversely proportional to the speed of sound, is decreased as described in equations given in Section 2.3. Therefore, the solution requires use of smaller time step increments to maintain numerical stability, resulting in higher computational cost. Still, the penalty stiffness based explicit solution results are a good approximation to the exact surface contact solution as studied by (Carpenter 1991).

2.2 Constitutive material model

In shot peening process, the target material Alum 2618-T61 is subjected to localized plastic deformation at high strain rates of the order of 10^5 s^{-1} (Meguid *et al.* 2002). Therefore, the target's material constitutive model should be capable to describe not only the material's work hardening but also the strain rate dependency of the flow stress during its plastic deformation. Such behaviour of metallic materials is widely elucidated by Johnson-Cook (Johnson and Cook 1983) model given as

$$\sigma = [A + B \varepsilon_p^n] \left[1 + C \ln \frac{\dot{\varepsilon}_p}{\dot{\varepsilon}_0} \right] \left[1 - \left(\frac{T - T_0}{T_{melt} - T_0} \right)^m \right] \quad (1)$$

where ε_p is equivalent plastic strain, $\dot{\varepsilon}_p$ and $\dot{\varepsilon}_0$ are the applied and reference strain rates, T , T_0 and T_{melt} are applied, reference and melting temperature, A is the material initial yield strength, B and n are work hardening modulus and exponent, respectively, C and m are constants describing the flow stress dependency on strain rate and temperature. In present simulations, the thermal effects are neglected as the shot peening is usually considered as cold working process (Hassani-Gangaraj and Schuh 2015) and

Table 1 Material properties of shot and target plate

Property	Target Plate Alum 2618 -T61	Shot Material Steel
Density (Kg/m ³)	2760	8000
Young's Modulus (GPa)	71.7	200
Poisson's ratio	0.33	0.3
Yield Strength ,A,(MPa)	330	
B (MPa)	480	
C	0.02	
n	0.45	
$\dot{\varepsilon}_0$	1.0	

hence parameter 'm' is taken as zero. Parameters of Johnson-Cook model are usually determined through experimental testing of material at high strain rates. In this study, initially the parameters were selected from literature (Hfaiedh *et al.* 2015) for aluminium alloys. However, in final simulations, the constants A, B and n were calibrated numerically by obtaining a close fit between numerical and experimental true stress-strain curves. The rate dependent properties were taken from the literature for similar material. These constants along with target elastic properties are listed in Table 1. Steel shot was modelled as linear elastic material with properties given in Table 1.

2.3 Elements, mesh sensitivity and explicit solution technique

An 8-noded linear Solid 164 hexahedron element specific for explicit dynamics analyses was used for meshing both the shot and target plate. The element has degrees of freedom of translations, velocities, and accelerations at each node in the x, y, and z directions (2015). The element was defined with reduced integration and viscous hourglass control options. Reduced integration is beneficial in saving the computational time in cases of high nonlinearities. Further, these options have the capability of controlling hourglass and eliminate the occurrence of shear locking in problems where the bending effect is dominant. Lagrangian formulation option was selected to elucidate the material as a continuum.

A realistic mesh density is required to capture the residual stress and plastic deformation along the surface and depth of the target plate. Therefore, three different FE models were developed to achieve the mesh convergence, using different mesh sizes in the plane as well as depth of the target plate. Both the plate and shot were mapped meshed in all the models. A biased meshing scheme was adopted with finer mesh at the shot impact location on the target top surface. This biasing was also defined along the plate depth with finer mesh at the top and coarser at the bottom. FE models with three meshes I, II and III resulted in

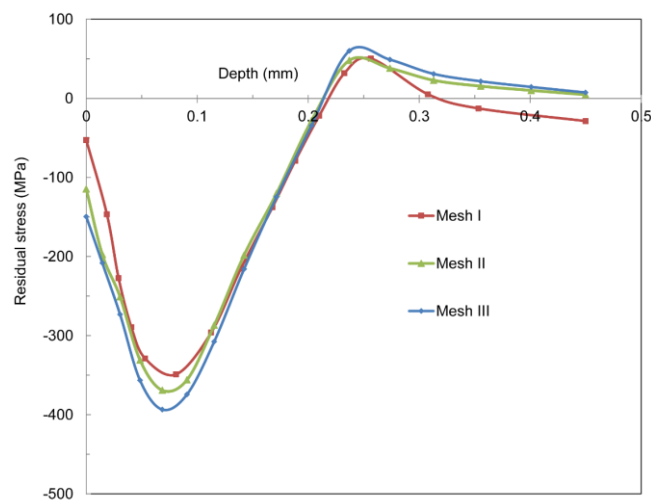


Fig. 2 Mesh sensitivity - residual stress along the depth of target

3168, 11840, 32256 elements, respectively. The shot mesh size was kept the same in all the models. These models were solved for 10 μ s with impact velocity of 50 m/s. Results of these three models are compared in Fig. 2 showing residual stress distribution along the target depth. Here, mesh convergence was achieved with FE model of mesh II, which was selected for subsequent simulations of shot peening process with lesser computational cost.

To simulate high velocity transient problems involving large deflections, material nonlinearities and contact interactions, an explicit dynamics analysis technique is usually employed. Explicit scheme is more efficient than the implicit one, and for high velocity impact can be more accurate. However, the stability of explicit scheme is dependent on the time step size, i.e., smaller the time step the more stable the solution is. This requires that the information should not propagate more than one element during a single time step. Thus, a smaller time step increases the total computational time for transient loading. Hence, in a dynamic analysis, the required time step is very short compared to a static one, as capturing of the stress waves moving at high speed in the FE model is an essential requirement. The stable time increment of the whole model is defined by its smallest element. The calculated time step for the transient analysis is therefore analogous to the time required for the stress wave to cross the smallest element in the model. The stable time increment ΔT as described in (Carlberger 2007, Ullah 2015), can be defined in terms of the wave speed of the material, C_d , and element length, L_e , as $\Delta T = L_e / C_d$, where $C_d = \sqrt{E/\rho}$, E is the Young's modulus and ρ is the density of the material. The wave speed in the aluminium plate is 5060 m/s. Based on the smallest element size of 14.3 μ m in the target plate, the stable time increment is 2.83×10^{-9} seconds from the above relation. The stable time increment calculated automatically by LS/Dyna solver is 1.31×10^{-9} seconds, which is less than the critical value of 2.83×10^{-9} seconds, thus satisfying the criterion for explicit dynamics solution of the problem. The total simulation time was fixed at 10 μ s. This longer computation time, as compared to the steel shot impact duration of 1.08 μ s, was selected to capture the residual behaviour of the target material after impact. In order to capture the shot impact process, a small time increment of 1.31×10^{-9} s was used for the initial velocity to be applied gradually.

2.4 Model validation

The numerical study of Meguid *et al.* (Meguid *et al.* 1999) was used as a reference for validation of the modelling procedure. They conducted numerical analysis of 1 mm diameter rigid steel shot impacted at 75 m/s on a high strength steel target of size $3.5 \times 2.5 \times 2.0$ mm³. The target plate had 600 MPa yield strength and a tangent modulus of 800 MPa. In this study, an FE model based on these geometric and material properties was built in Ansys/LS Dyna with the element type, contact interaction and boundary conditions described above. Comparison of the present study with deformable shot and Meguid *et al.* (Meguid *et al.* 1999) with rigid shot is presented in Fig. 3 showing the variation of residual stress with depth along the

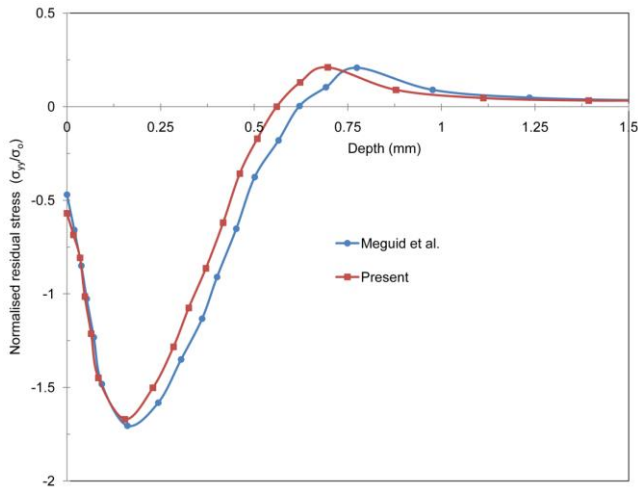


Fig. 3 Numerical validation of shot impact

target centreline. There is a fair agreement between the results, thus validating the present FE modelling approach. It can be observed from Fig. 3 that there is a negligible difference in the maximum residual stress obtained with both types of shot modelling approaches. However, the depth of compressive residual stress i.e., zero-crossing of the stress profile is slightly more with rigid shot (Meguid's study) than deformable one (Present study). Since in deformable shot impact, the shot also deforms apart from the target and hence causes lesser penetration in the target than rigid shot. Further, as already described that stiffness of the shot is larger than that of the target, thus the effect of deformable shot is similar to that of rigid one. These findings are also corroborated by simulation studies of (Guagliano 2001) and (Mylonas and Labeas 2011), who showed that results obtained using a deformable elastic shot are close to those obtained with a rigid shot. This conclusion can be generalised to low stiffness and hardness materials such as aluminium alloys impacted with high stiffness and hardness steel shots.

2.5 Parametric study

As elaborated earlier that various parameters such as shot velocity, diameter and material of both the shot and target are involved in peening process to achieve the desired level of plastic deformation and residual stresses in a part. Experimental prediction of these parameters is not only costly but time consuming as well. Therefore, a parametric study was conducted employing FE models to assess the influence of various parameters upon the residual stress distribution and permanent plastic deformation. In these models, the effect of shot velocity was evaluated by using 20, 50, 75 and 100 m/s velocity. The effect of shot size was studied by developing models with shot diameters of 400 μm , 1.0 mm and 2.0 mm. Such data obtained can be very useful in proper selection and control of shot peening parameters.

3. Results and discussion

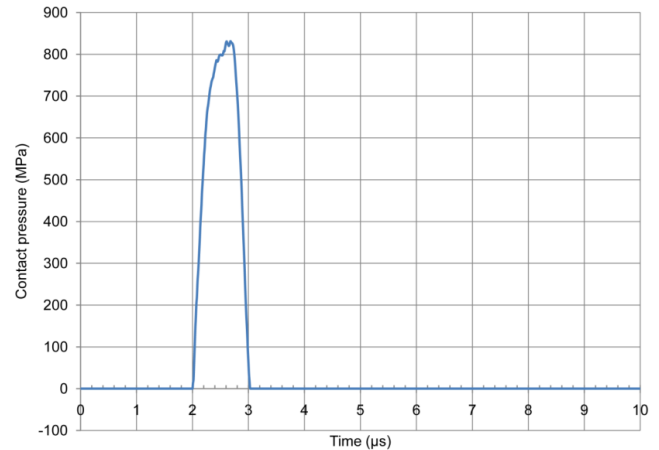


Fig. 4 Variation of contact pressure over time

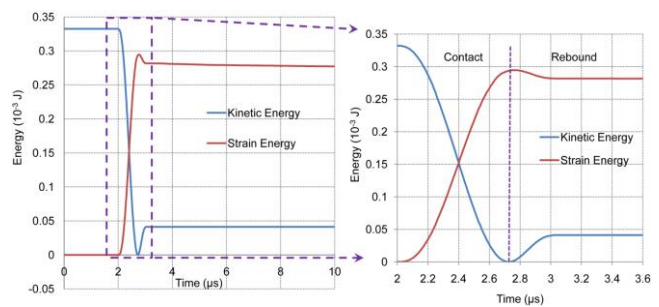


Fig. 5 Variation of the model energy over time

Results of numerical simulations for the shot peening induced impacts by using the steel shots on aluminium target are presented in this section. Here, first the transient response of impact process is elaborated in terms of force and energy time histories as well as distributions of stress and equivalent plastic strain at various time intervals. The indentation shapes resulted from the shot impingements are also compared. These results are illustrated for shots of 400 μm diameter impacting the aluminium target at 50 m/s velocity. Subsequently, the results of parametric study and its effects on the resulting residual stress profiles and plastic deformation are summarised.

The transient response of the steel shot impact on the target plate in terms of contact pressure vs. time is shown in Fig. 4. As the contact engaged between the shot and plate, the pressure increased till some fluctuations occurred before the peak pressure was reached. These fluctuations or pressure drops represent the local plastic deformation of the plate caused by the high velocity shot. After reaching the peak, the shot bounced back and the contact pressure dropped to zero. The pressure peak reached to 826 MPa with total impact duration of 1.08 μs . During the impact process, the energy variation of both the shot and plate is presented in Fig. 5. The impact process consisted of two stages: the contact process and the rebound process. As the shot was kept at a distance from the plate, it took 2 μs to reach the target. The contact then started at 2 μs , where the shot kinetic energy started decreasing till it reached zero at 2.72 μs , while the plate's strain energy increased till its peak value. After this point, some of the strain energy stored by the plate was transferred back to the shot's kinetic energy,

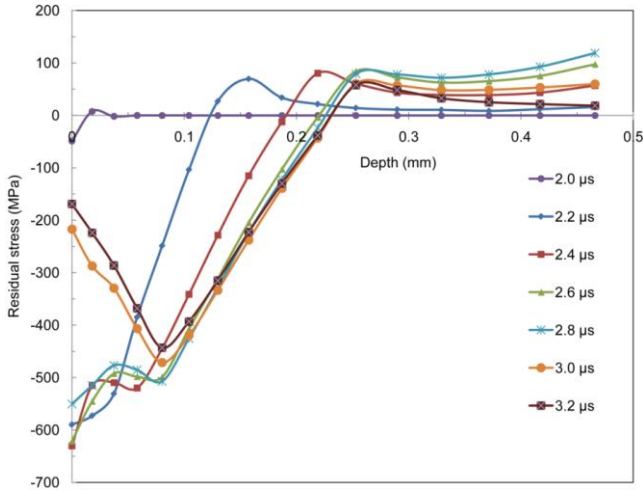


Fig. 6 Distribution of Z-stress along the centre-line of the plate beneath the contact point at different times

thus causing its rebound till $3.08 \mu\text{s}$. The difference in shot maximum kinetic energy and the plate peak strain energy is the energy mainly dissipated due to plastic deformation of the plate apart from small amount of frictional dissipation.

In the contact process, the stress waves also start to propagate in the target. To analyse the propagation of these waves, the distribution of the stress parallel to the plate surface (z-direction) at the contact point beneath the shot along the centre-line of the plate and its contour plots at different times are shown in Figs. 6 and 7, respectively. In the contact process, with the increase in the strain energy and plastic dissipated energy, both the surface compressive stress and the penetration depth increase. As the shot impacts the plate at $2 \mu\text{s}$, compressive stress is developed in the plate. At $2.2 \mu\text{s}$, the compressive stress increases till its max value of 680 MPa beneath the shot at $2.6 \mu\text{s}$. Fig. 7 shows a higher value of 767 MPa at this interval, but this is away from the central contact point. These magnitudes of compressive stresses are higher than 330 MPa tensile yield strength of the target. This shows that large hydrostatic compressive stresses are induced by the impact of the high speed shots apart from deviatoric ones. The compressive stressed regions, which are green and blue plastically deformed, are surrounded by elastic tensile stressed regions shown by red contours in Fig. 7. After rebound of shot at $2.72 \mu\text{s}$, the magnitude of the stress starts to reduce till $3.08 \mu\text{s}$. After this time interval, the compressive stresses left in the plate were the residual stresses on the plate surface caused by impact. At $3.2 \mu\text{s}$, the surface and subsurface residual stresses are 170 MPa and 434 MPa , respectively, shown in Figs. 6 and 7. The maximum compressive residual stress 432 MPa is located at a depth of $85 \mu\text{m}$, and the total depth of the compressive residual stress layer is $230 \mu\text{m}$ as shown in Fig. 6. By using an explicit solver, the analysis was purely dynamic and hence the residual stress oscillated about a mean value even during impact (see plots for 2.0 - $2.6 \mu\text{s}$ in Fig. 6). The equivalent plastic strain in the target plate at the contact point beneath the shot along the centre-line of the plate at different times is shown in Fig. 8. Both the magnitude and depth of the plastic strain increased till

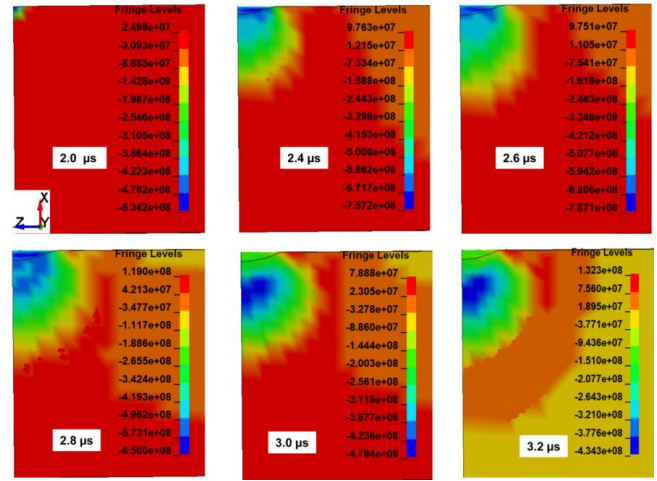


Fig. 7 Contours of Z- stress (Pascal) distribution along the centre-line of the plate beneath the contact point at different times

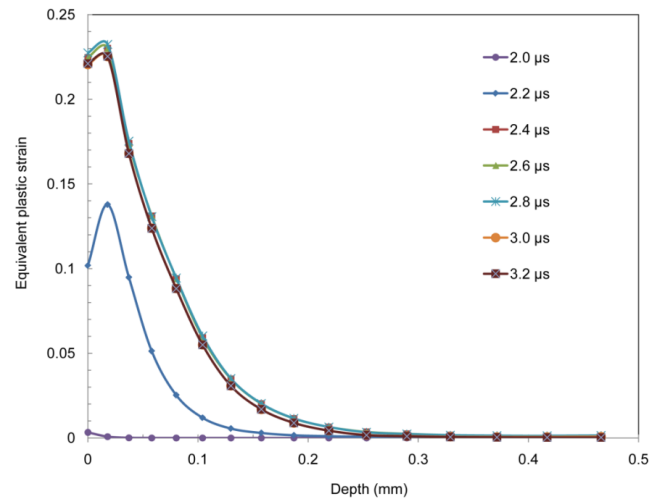


Fig. 8 Distribution of equivalent plastic strain along the centre-line of the plate beneath the contact point at different times

rebound of shot. The maximum equivalent plastic strain appeared below the top surface of the plate and then decreased gradually along the depth direction. After rebound at $3.2 \mu\text{s}$, permanent plastic strain existed below the top surface of the target with a total depth of $240 \mu\text{m}$. It is interesting to note that the depth of the strain-hardened layer is nearly the same as the depth of maximum residual compressive stress. Such a result is in good agreement with the previous study of shot peening in (Dai and Shaw 2007). The distributions of plastic strains along the plate thickness are further highlighted in Figs. 10 and 12.

Fig. 9 shows the indentation shapes obtained from impact of steel shot of $400 \mu\text{m}$ diameter at 50 m/s velocity and their comparison with indentation shapes from reference (Mann *et al.* 2015). Fig. 9(a) represents the coordinate system and the indentation (deformation u_x) contours showing dimple at the impact centre of the shot. Fig. 9(b) shows the indentation shape obtained numerically. The dimple diameter at the target surface and impingement

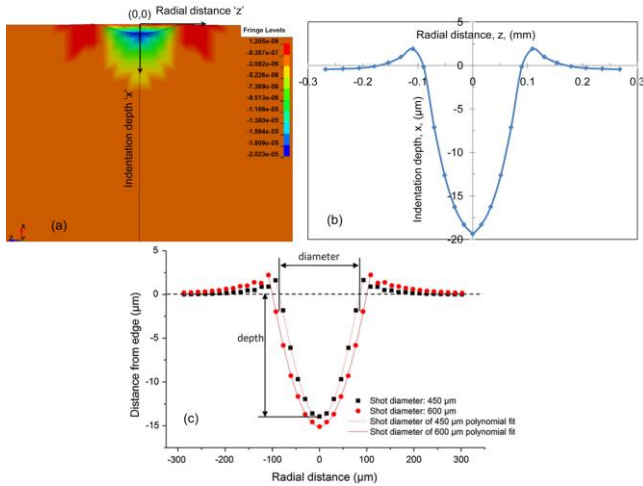


Fig. 9 Indentation shapes: (a) cross-sectional contour of deformation from 400 μm diameter shot impact at 50 m/s velocity, (b) indentation shape from present study, (c) indentation shape obtained with shots of 450 μm and 600 μm diameters at velocity of 54 m/s from (Mann *et al.* 2015)

depth can be computed from the indentation profile. The steel shot resulted in 180 μm dimple diameter with approximately 20.0 μm depth. The profile, dimple diameter and impingement depth obtained for steel shot are comparable with those presented in Fig. 9(c) taken from (Mann *et al.* 2015), where a ceramic shot of diameter 450 μm is impacted at 54 m/s on an aluminium AA2024-T35 plate. In (Mann *et al.* 2015), the impingement diameter and depth obtained numerically were within 3% of that measured experimentally. Therefore, validation of FE model and simulation technique developed in this study is further corroborated by this comparison of simulation and experimental results.

3.1 Effect of shot velocity

The effect of shot velocity on the maximum residual stress and equivalent plastic strain along z -direction (parallel to the surface) against the plate thickness below impact centre is presented in Fig. 10. It is evident that the variation in magnitude of maximum subsurface residual stress is negligible with increasing velocity. The maximum residual stress ranges from 400 MPa to 440 MPa for both types of shots. The reason is that the compressive residual stress development is mainly related to the mechanical properties of the target material. However, the total depth of compressive residual stress i.e., zero-crossing of the stress profile increases with increase in velocity. An increase in beneficial depth which corresponds to maximum subsurface residual stress can also be observed in Fig. 10. Here, it is worth mentioning that the maximum residual stress calculated for each shot type should be examined together with the plastic deformation presented in Fig. 10(b), for better understanding the influence of shot velocity on target material's behaviour. The maximum equivalent plastic strain increased linearly with increasing velocity i.e., the increased shot velocity and kinetic energy for constant

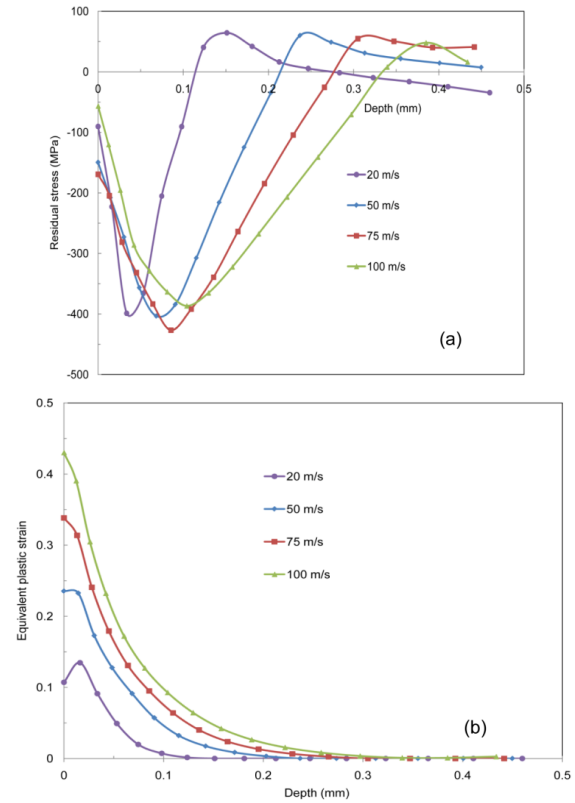


Fig. 10 Effect of shot velocity on (a) residual stress and (b) equivalent plastic strain

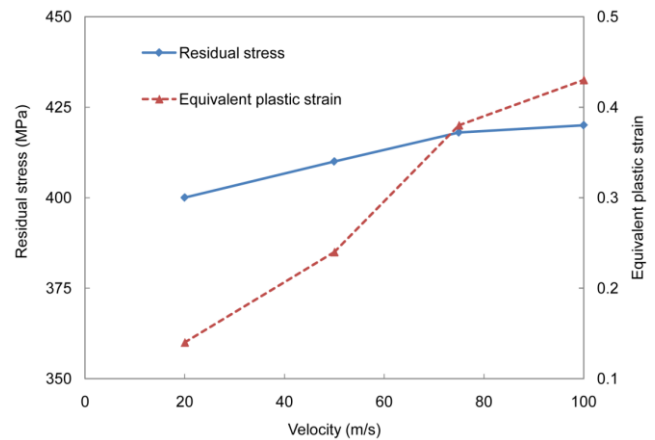


Fig. 11 Effect of shot velocity on maximum residual stress and equivalent plastic strain

shot's mass induced larger plastic deformation. The effect of shot's velocity on target's behaviour is further elaborated in Fig. 11, where the maximum subsurface residual stress and maximum equivalent plastic strain is plotted against the shot velocity. As stated earlier, the residual stress is changing negligibly with increasing velocity, whereas the maximum equivalent plastic strain along with its depth increases substantially with increase in velocity. The obtained plots are very useful to identify velocity of shots for required level of residual stress and plastic deformation zone in aluminium plates. Similar profiles and trends of residual stress and equivalent plastic strain distributions for

varying the impact velocity have been reported in (Guagliano 2001, Dai and Shaw 2007, Mylonas and Labeas 2011, Chen *et al.* 2014).

3.2 Effect of shot size

As increasing the shot diameter for constant initial velocity, the kinetic energy is increased with increase in shot's mass. Hence, more energy is transferred to the target inducing larger zone of plastic deformation. The effect of shot size on the residual stress profile as well as equivalent plastic strain at constant velocity of 50 m/s is illustrated in Fig. 12. It can be observed that despite increasing the shot diameter inducing plastic deformation in larger volume, the magnitude of maximum subsurface residual stress remained almost the same. But both the beneficial depth at maximum residual stress and total depth at zero residual stress increased linearly with shot size. However, maximum equivalent plastic strain along with its depth increased with increase in shot size. Similar trends of residual stress and plastic deformation for various shot sizes have been reported in (Meguid *et al.* 1999, Guagliano 2001). The effect of shot's size on plate's behaviour is further illustrated in Fig. 13, where the maximum subsurface residual stress

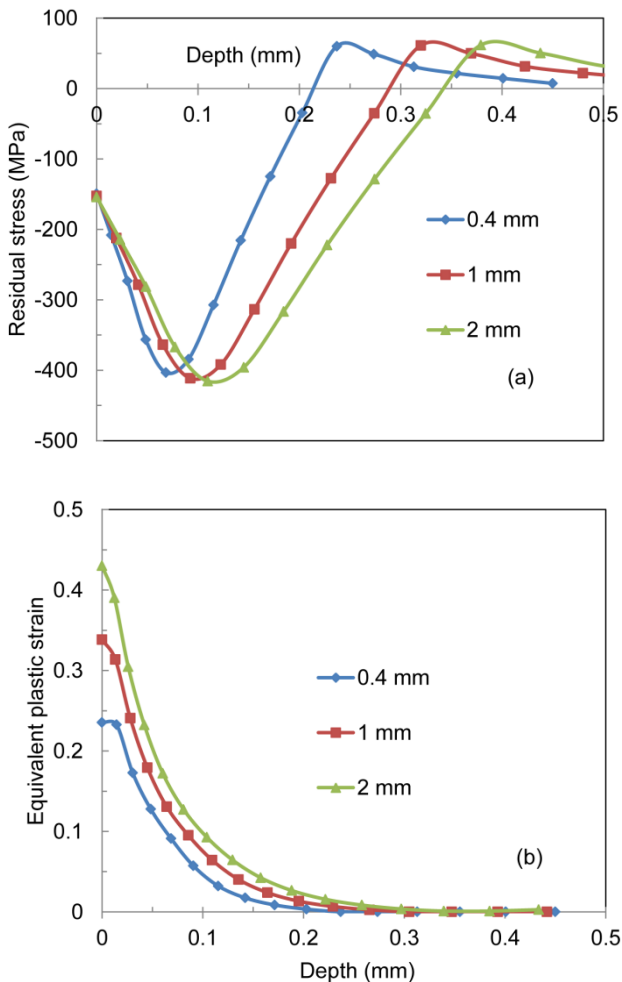


Fig. 12 Effect of shot diameter on (a) residual stress and (b) equivalent plastic strain

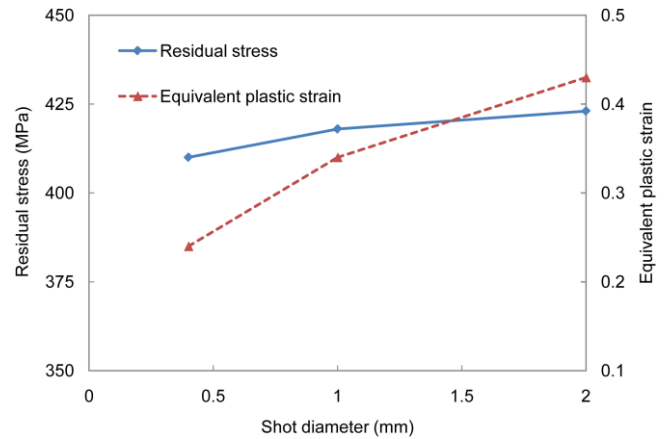


Fig. 13 Effect of shot size on maximum residual stress and equivalent plastic strain

and maximum equivalent plastic strain are plotted against the shot diameter. Again, the residual stress remains almost the same with increasing shot diameter, whereas the maximum equivalent plastic strain shows a substantial increase with increase in shot diameter. Both Figs. 12 and 13 can be used to specify size of shots for required level of residual stress and plastic strain in aluminium plates.

4. Conclusions

Finite element 3D models consisting of an elasto-plastic aluminium alloy target plate and elastic steel shots were developed in explicit dynamics solution code LS/Dyna to simulate shot peening process. The strain rate dependent constitutive behaviour of target plate was described by Johnson-Cook's plasticity model. The modelling procedure and simulation results were validated with published data. It was observed from comparison that both deformable and rigid shot models yielded similar results. The time histories of contact pressure, model energies and distributions of stress and plastic deformation elaborated the dynamic behaviour of the peening process. The obtained numerical results were in accordance with the published ones, and the numerical models demonstrated their capability to simulate the pattern of residual stress and plastic deformation observed experimentally in aluminium alloys. The numerical models enhanced understanding of the complex impact process and parametric study investigated the relationship among various factors involved. It was observed that higher the shot velocity, larger is the depth of residual stress i.e., resulted in larger plastic zone in target plate. Further, increasing the shot size resulted in an increase in plastic deformation. However, the maximum subsurface residual stress was negligibly influenced by the shot velocity and size. In industry, the study can be used to select a proper set of peening parameters for specific levels of residual stress and plastic deformation in aluminium alloy components especially aero engine compressor blades. Such data seems to be very difficult to be obtained with experimentation. In future, effect of multiple shots impact at various oblique angles will be studied.

References

- Al-Obaid, Y. (1990), "Three-dimensional dynamic finite element analysis for shot-peening mechanics", *Comput. Struct.*, **36**(4), 681-689.
- ANSYS LS-DYNA User's Guide (2015)
- Bhuvanaraghan, B., Srinivasan, S.M., Maffeo, B., McClain, R.D., Potdar, Y. and Prakash, O. (2010), "Shot peening simulation using discrete and finite element methods", *Adv. Eng. Softw.*, **41**(12), 1266-1276.
- Bagherifard, S., Ghelichi, R. and Guagliano, M. (2014), "Mesh sensitivity assessment of shot peening finite element simulation aimed at surface grain refinement", *Surface Coat. Technol.*, **243**, 58-64.
- Rubio-Gonzalez, C., Gomez-Rosas, G., Ruiz, R., Nait, M. and Amrouche, A. (2015), "Effect of laser shock peening and cold expansion on fatigue performance of open hole samples", *Struct. Eng. Mech.*, **53**(5), 867-880.
- Chen, Z., Yang, F. and Meguid, S.A. (2014), "Realistic finite element simulations of arc-height development in shot-peened almen strips", *J. Eng. Mater. Technol.*, **136**(4), 041002.
- Mylonas, G.I. and Labeas, G. (2011), "Numerical modelling of shot peening process and corresponding products: residual stress, surface roughness and cold work prediction", *Surface Coat. Technol.*, **205**(19), 4480-4494.
- Johnson, G.R. and Cook, W.H. (1983), "A constitutive model and data for metals subjected to large strains, high strain rates and high temperatures", *Proceedings of the 7th International Symposium on Ballistics*, The Hague, The Netherlands.
- Guagliano, M. (2001), "Relating Almen intensity to residual stresses induced by shot peening: a numerical approach", *J. Mater. Proc. Technol.*, **110**(3), 277-286.
- Hassani-Gangaraj, S.M., K.S. Cho, H.J.L. Voigt, M. Guagliano and C.A. Schuh (2015), "Experimental assessment and simulation of surface Nanocrystallization by severe shot peening", *Acta Materialia*, **97**, 105-115.
- Hfaiedh, N., Peyre, P., Song, H., Popa, I., Ji, V. and Vignal, V. (2015), "Finite element analysis of laser shock peening of 2050-T8 aluminum alloy", *Int. J. Fatigue*, **70**, 480-489.
- Hidayetoglu, T.K. (2001), "Effect of the gear finishing process on bending fatigue crack initiation and propagation in spur gears", *Proc. Inst. Mech. Engineers, Part C: J. Mech. Eng. Sci.*, **215**(7), 785-792.
- Hong, T., Ooi, J. Y. and Shaw, B. (2008), "A numerical simulation to relate the shot peening parameters to the induced residual stresses", *Eng. Fail. Anal.*, **15**(8), 1097-1110.
- Hong, T., Ooi, J.Y. and Shaw, B.A. (2008), "A three-dimensional finite element analysis of two/multiple shots impacting on a metallic component", *Struct. Eng. Mech.*, **29**(6), 709-729.
- Jack Hetherington, A.R.F. and Harm Askes (2011), "Controlling the critical time step with the bi-penalty method", *OMPDYN 2011, 3rd ECCOMAS Thematic Conference on Computational Methods in Structural Dynamics and Earthquake Engineering*, M. F. M. Papadrakakis, V. Plevris Greece.
- Dai, K. and Shaw, L. (2007), "Comparison between shot peening and surface nanocrystallization and hardening processes", *Mater. Sci. Eng.: A*, **463**(1), 46-53.
- Majzoobi, G.H., Azizi, R. and Nia, A.A. (2005), "A three-dimensional simulation of shot peening process using multiple shot impacts", *J. Mater. Proc. Technol.*, **164**, 1226-1234.
- Mann, P., Miao, H.Y., Gariépy, A., Lévesque, M. and Chromik, R.R. (2015), "Residual stress near single shot peening impingements determined by nanoindentation and numerical simulations", *J. Mater. Sci.*, **50**(5), 2284-2297.
- Meguid, S. and L.A. Maricic (2015), "Finite element modeling of shot peening residual stress relaxation in turbine disk assemblies", *J. Eng. Mater. Technol.*, **137**(3), 031003.
- Meguid, S.A., Shagal, G. and Stranart, J.C. (2002), "3D FE analysis of peening of strain-rate sensitive materials using multiple impingement model", *Int. J. Impact Eng.*, **27**(2), 119-134.
- Meguid, S.A., Shagal, G., Stranart, J.C. and Daly, J. (1999), "Three-dimensional dynamic finite element analysis of shot-peening induced residual stresses", *Finite Element. Anal. Des.*, **31**(3), 179-191.
- Mohamed Jebahi, A.G., Julie Levesque, Oussama Mechri and Kadiata, B.A. (2016), "Robust methodology to simulate real shot peening process using discrete-continuum coupling method", *Int. J. Mech. Sci.*, **107**, 21-33.
- Nicholas, J., Carpenter, R.L.T. and Michael G. Katona (1991), "Lagrange constraints for transient finite element surface contact", *Int. J. Numer. Method. Eng.*, **32**(1), 103-128.
- Shukla, P.P., Swanson, P.T. and Page, C.J. (2014), "Laser shock peening and mechanical shot peening processes applicable for the surface treatment of technical grade ceramics: A review", *Proc. Inst. Mech. Engineers, Part B: J. Eng. Manufact.*, **228**(5), 639-652.
- Belytschko, T. and Neal, M.O. (1991), "Contact-impact by the pinball algorithm with penalty and Lagrangian methods", *Int. J. Numer. Method. Eng.*, **31**(3), 547-572.
- Carlberger, T. and Stigh, U. (2007), "An explicit FE-model of impact fracture in an adhesive joint", *Eng. Fract. Mech.*, **74**(14), 2247-2262.
- Ullah, H. and Silberschmidt, V.V. (2015), "Numerical analysis of the interactive damage mechanisms in two-dimensional carbon fabric-reinforced thermoplastic composites under low velocity impacts", *J. Compos. Mater.*, **49**(25), 3127-3143.

PL